Quantifying the causal strength of multivariate cardiovascular couplings with momentary information transfer

2015 Physiol. Meas. 36 813

(http://iopscience.iop.org/0967-3334/36/4/813)

IOP Publishing | Institute of Physics and Engineering in Medicine Physiological Measurement

Physiol. Meas. **36** (2015) 813–825 doi:10.1088/0967-3334/36/4/813

Quantifying the causal strength of multivariate cardiovascular couplings with momentary information transfer

Jakob Runge[1,2], Maik Riedl[1,2], Andreas Müller[1], Holger Stepan[3], Jürgen Kurths[1,2,5] and Niels Wessel[1,4]

[1] Department of Physics, Humbolt University Berlin, Berlin, Germany
[2] Potsdam Institute for Climate Impact Research, Potsdam, Germany
[3] Department of Obstetrics and Gynaecology, University of Leipzig, Leipzig, Germany
[4] Sleep Center, Charité University Hospital, Berlin, Germany
[5] Institute for Complex Systems and Mathematical Biology, University of Aberdeen, Aberdeen, United Kingdom

E-mail: jakobrunge@gmail.com

Received 3 October 2014, revised 15 December 2014
Accepted for publication 18 December 2014
Published 23 March 2015

Abstract

This article studies a recently introduced information-theoretic approach to detect and quantify the causal couplings in a complex cardiovascular system. In the first step a causal algorithm detects the coupling delays and in the second step the causal strength of each coupling mechanism is quantified using the recently introduced momentary information transfer. As an example, the method is applied to time series of respiration, systolic and diastolic blood pressure, and heart rate of pregnant healthy women and women suffering from pre-eclampsia. A possible explanation for the influence of heart rate on systolic blood pressure is found and some differences between healthy women and patients are discussed.

Keywords: causality, information theory, pre-eclampsia, baroreflex

(Some figures may appear in colour only in the online journal)

1. Introduction

Complex interactions in the cardiovascular system have been studied using model-based approaches as well as by applying various coupling measures, starting from cross correlation and spectral methods via mutual predictability and sequence statistics to information-theoretic methods (Granger 1969, Cohen and Taylor 2002, Porta *et al* 2002, Rosenblum *et al* 2002,

Paluš and Stefanovska 2003, Laude *et al* 2004, Nollo *et al* 2005, Cammarota and Rogora 2006, Faes *et al* 2006, Schelter *et al* 2006, Marwan *et al* 2007, Paluš and Vejmelka 2007, Dhamala *et al* 2008, Leistritz *et al* 2013, Schulz *et al* 2013, Stankovski *et al* 2013, Bopp *et al* 2014). Probably the most prominent coupling in the cardiovascular system is the so-called baroreflex, which is the change of the heart rate in response to the increase and decrease of systolic blood pressure. The diagnostic relevance of the baroreflex sensitivity has been proven in many studies, such as in Malberg *et al* (2007) where this parameter and two others were used to improve the standard diagnostic tool of *pre-eclampsia* (Doppler sonography). This serious disorder is characterized by hypertension (mean systolic/diastolic blood pressure greater than 140/90 mmHg) and proteinuria of more than 300 mg a day during the third trimester of pregnancy. Laude *et al* (2004) studied this interaction using bivariate sequence statistics. Most of the above-mentioned works are based on bivariate methods. A bivariate analysis has also been used to reconstruct the interaction between heart rate, systolic and diastolic blood pressure, and respiration in de Boer's beat-to-beat model of hemodynamic fluctuations and baroreflex sensitivity (deBoer *et al* 1987). However, the most critical problem of this bivariate analysis is the influence of the respiration on both heart rate and systolic blood pressure. Several different multivariate approaches have been used to overcome this, such as using Granger causality (Porta *et al* 2000). In particular, methods which take nonlinear behavior into account have given new results about the complex structure of such an interaction. For example, Riedl *et al* (2010) found the same coupling pattern in both healthy pregnant women and patients suffering from pre-eclampsia. The patterns include the influence of respiration on heart rate, systolic blood pressure, and diastolic blood pressure, the influence of heart rate on diastolic blood pressure, and the effect of diastolic blood pressure on systolic blood pressure. The only difference was found in the morphologies of the couplings in both groups. Surprisingly, the authors did not detect a coupling of heart rate and systolic blood pressure, which led them to the conclusion that the baroreflex in pregnant women measured by Malberg *et al* (2007) results from the simultaneous influence of respiration on both heart rate and blood pressure.

The approach in Riedl *et al* (2010) was still based on a (nonlinear) model. Here we study the interactions in the model-free framework of information theory. This overcomes the possibility of a misspecified model in an assessment of causal interactions. On the other hand, model-based approaches can yield more insights into the functional form of a dependency, as discussed in Riedl *et al* (2010), and are typically better estimable. The most straightforward way to generalize the Granger causality in an information-theoretic framework is via transfer entropy (Schreiber 2000). As analyzed in Runge *et al* (2012b), the drawback of this approach is that it does not include causal lags and it suffers from the curse of dimensionality, which is why it has mostly been used in a bivariate setting. Here we study the causal interactions for the general multivariate case, including causal lags, using the theory of graphical models adapted to time series (Runge *et al* 2012b). We also utilize information-theoretic measures to address a second goal: measuring the strength in a meaningful way (Runge *et al* 2012a). This novel approach is compared with lagged mutual information, transfer entropy, and symbolic coupling traces (Wessel *et al* 2009) on a dataset of pregnant healthy women and women suffering from pre-eclampsia. One important result is that a multivariate analysis unveils the influence of heart rate on systolic blood pressure as only indirectly mediated via diastolic blood pressure. This finding indicates a flaw in the extraction of baroreflex sensitivity by means of standard bivariate sequence methods and spectral approaches based on high frequency power (Laude *et al* 2004).

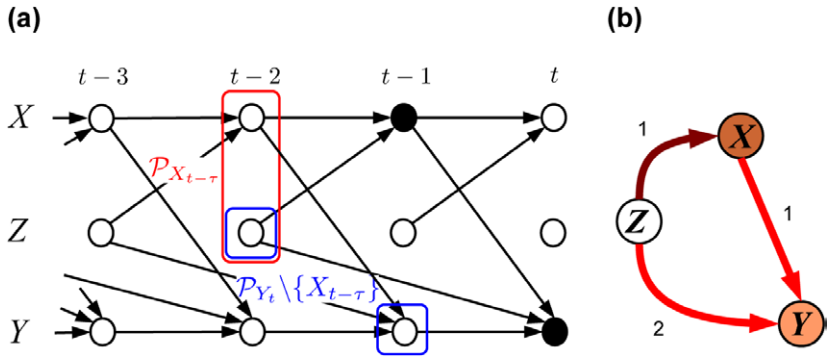

Figure 1. Causal interactions in a multivariate process $\mathbf{X}$. (*a*) Example of a time series graph (see definition in text). Note that stationarity implies that '$X_{t-\tau} \to Y_t$' whenever '$X_{t'-\tau} \to Y_{t'}$' for any t'. The set of *parents* $\mathcal{P}_{Y_t}$ (blue boxes) separates Y_t from the past of the whole process $\mathbf{X}_t^- \setminus \mathcal{P}_{Y_t}$, which is used in the algorithm to estimate the graph. Here MIT between X_{t-1} and Y_t (black dots) is the conditional mutual information conditional on both the parents of X_{t-1} (red box) and Y_t (blue boxes). (*b*) Process graph, which aggregates the information in the time series graph for better visualization (the labels denote the lags, the link colors encode the MIT strength, and the node colors denote the autodependency MIT strength).

2. Method

2.1. Conditional mutual information

Information theory provides a genuine framework for the model-free study of couplings among time series. Mutual information (MI) and its conditional extension *conditional mutual information* (CMI) are well-known information-theoretic functionals (Cover and Thomas 2006). CMI is defined using Shannon entropies H as

$$I(X;Y|Z) \equiv H(Y|Z) - H(Y|X,Z) \tag{1}$$

which can be phrased as the decrease in uncertainty about Y given Z if additionally X is known. CMI can be used to assess (Granger) causality because it is zero if and only if X and Y are independent *conditionally on* Z. In figure 1(*b*) the CMI $I(X;Y|Z)$ would be zero if there was no link $X \to Y$ but the mutual information $I(X;Y)$ would still be non-zero due to the common driver Z. Instead of the commonly used binning estimators, here we use an advanced nearest-neighbor estimator (Frenzel and Pompe 2007) that is most suitable for variables taking on a continuous range of values. This estimator has as a free parameter for the number of nearest-neighbors k, which determines the size of hyper-cubes around each (high-dimensional) sample point. Small values of k lead to a lower estimation bias but higher variance, and vice versa. Note that stationarity is required for an estimation from a (multivariate) time series.

2.2. Time series graphs

The present discussion has not included the important aspect of causal lags or delays, which are crucial to determine causal interactions in time series, as initiated by the works of Granger. The more detailed time-resolved picture in figure 1(*a*) shows that, given $X_{t-1} \to Y_t$ does not exist, X_{t-1} and Y_t are *not* independent given only the common driver Z_{t-2} as a condition. Rather, additionally Y_{t-1} needs to be included in the conditions to exclude all of the

paths connecting the two. These subtle interactions can be captured with time series graphs stemming from the theory of graphical models. In the graphical model approach the conditional independence properties of a multivariate process are visualized in a graph, which are called *time series graphs* (Dahlhaus 2000, Eichler 2012) for the case of time-ordered data. Figure 1(*a*) shows an example. Each node in a time series graph represents a subprocess of a multivariate discrete time process $\mathbf{X}$ at a certain time t. Subprocesses/nodes $X_{t-\tau}$ and Y_t for $\tau > 0$ are connected by a directed link '$X_{t-\tau} \to Y_t$' if

$$I\left(X_{t-\tau}; Y_t | \mathbf{X}_t^- \setminus \{X_{t-\tau}\}\right) > 0, \tag{2}$$

i.e. if they are not independent conditionally on the past of the whole process, which implies a lag-specific Granger causality with respect to $\mathbf{X}$. If $Y \neq X$, then we say that the link '$X_{t-\tau} \to Y_t$' represents a *coupling at lag* τ, while for $Y = X$ it represents an *autodependency at lag* τ. Since contemporaneous associations—even so not causal—are also often of interest, we also define the links between X_t and Y_t by

$$I\left(X_t; Y_t | \mathbf{X}_{t+1}^- \setminus \{X_t, Y_t\}\right) > 0, \tag{3}$$

where the contemporaneous present $\mathbf{X}_t \setminus \{X_t, Y_t\}$ is also included in the condition. These links are marked by a straight line 'X_t–Y_t'. In the case of a multivariate autoregressive process, this definition corresponds to non-zero entries in the *inverse* covariance matrix of the innovations (Eichler 2012). In this graph the parents and neighbors of a node Y_t are defined as

$$\mathcal{P}_{Y_t} \equiv \{Z_{t-\tau} : Z \in \mathbf{X}, \tau > 0, Z_{t-\tau} \to Y_t\}, \tag{4}$$

$$\mathcal{N}_{Y_t} \equiv \{X_t : X \in \mathbf{X}, X_t - Y_t\}. \tag{5}$$

2.3. Causal algorithm

In Runge *et al* (2012b) an algorithm for the estimation of these time series graphs by iteratively inferring the parents is introduced. This algorithm is a modification of the PC algorithm (Spirtes and Glymour 1991, Spirtes *et al* 2000) (which is named after its inventors Peter Spirtes and Clark Glymour). The main idea is to iteratively unveil the links by testing for conditional independence between all possible pairs of nodes conditioned on iteratively more conditions and testing all of the combinations among them. Thereby, the dimension stays as low as possible in every iteration step. This important feature helps to alleviate the curse of dimensionality in estimating CMIs. The algorithm starts with no *a priori* knowledge about the links and iteratively learns the set of parents and neighbors for each Y:

For every Y, first we estimate unconditional dependencies $I(X_{t-\tau}; Y_t)$ and initialize the preliminary parents $\widetilde{\mathcal{P}}_{Y_t} = \{X_{t-\tau} : X \in \mathbf{X}, 0 < \tau \leqslant \tau_{\max}, I(X_{t-\tau}; Y_t) > 0\}$. This set contains also indirect links which are now iteratively removed by testing whether the dependence between Y_t and each $X_{t-\tau} \in \widetilde{\mathcal{P}}_{Y_t}$ conditioned on the incrementally increased set of conditions $\widetilde{\mathcal{P}}_{Y_t}^{n,i} \subseteq \widetilde{\mathcal{P}}_{Y_t}$ vanishes:

(n) Iterate n over increasing number of conditions, starting with some $n_0 > 0$:

n.1. Iterate i through all of the combinations of picking n nodes from $\widetilde{\mathcal{P}}_{Y_t}$ to define the conditions $\widetilde{\mathcal{P}}_{Y_t}^{n,i}$ in this step and estimate $I\left(X_{t-\tau}; Y_t | \widetilde{\mathcal{P}}_{Y_t}^{n,i}\right)$ for all $X_{t-\tau} \in \widetilde{\mathcal{P}}_{Y_t}$. After each

step the nodes $X_{t-\tau}$ with $I\left(X_{t-\tau}; Y_t|\widetilde{\mathcal{P}}^{n,i}_{Y_t}\right) = 0$ are removed from $\widetilde{\mathcal{P}}_{Y_t}$ and the i-iteration stops if all of the possible combinations have been tested.

If the cardinality $|\widetilde{\mathcal{P}}_{Y_t}| \leqslant n$, then the algorithm converges; else, increase n by one and iterate again.

Once the parents of each process are known, the same algorithm for $\tau = 0$ can be used to infer the contemporaneous neighbors $\mathcal{N}_{Y_t}$, where now undirected links are removed if $I\left(X_t; Y_t|\mathcal{P}_{Y_t}, \widetilde{\mathcal{N}}^{n,i}_{Y_t}, \mathcal{P}\left(\widetilde{\mathcal{N}}^{n,i}_{Y_t}\right)\right) = 0$.

2.4. Shuffle significance test

In Runge *et al* (2012b) a shuffle test is used for testing whether $I\left(X_{t-\tau}; Y_t|\widetilde{\mathcal{P}}^{n,i}_{Y_t}\right) > 0$. An ensemble of M values of $I\left(X^*_{t-\tau}; Y_t|\widetilde{\mathcal{P}}^{n,i}_{Y_t}\right)$ is generated where $X^*_{t-\tau}$ is a shuffled sample of $X_{t-\tau}$, i.e. with the indices permuted. Note that $t - \tau$ refers to lagged sequences and the CMI is estimated by averaging over time. If, however, a large enough ensemble from measurements from different subjects is available, then the time average can also be replaced by an ensemble average. Here, we use time-averaging. The CMI values are then sorted and for a test at a given α-level, the α M-th value is taken as a significance threshold. A numerical study on the detection and false positive rates of the algorithm is given in Runge *et al* (2012b).

2.5. Momentary information transfer

Time series graphs encode the existence of a lag-specific causality but they are not meant to assess the causal strength in a meaningful way. To this end, *momentary information transfer* (MIT) (Pompe and Runge 2011, Runge *et al* 2012a, Runge *et al* 2014) between X at some lagged time $t - \tau$ in the past and Y at time t is the CMI that measures the part of entropy of Y that is shared with the source entropy of X:

$$I^{\mathrm{MIT}}_{X\to Y}(\tau) \equiv I\left(X_{t-\tau}; Y_t|\mathcal{P}_{Y_t}\setminus\{X_{t-\tau}\}, \mathcal{P}_{X_{t-\tau}}\right). \tag{6}$$

MIT is well interpretable because it excludes past information, not only from Y but also from X. In figure 1(*a*) the MIT of the link $X \to Y$ can be better interpreted than the MI $I(X;Y)$ because it excludes common information due to Z that obscures the strength of the actual coupling mechanism between X and Y. As is demonstrated analytically and numerically in Runge *et al* (2012a), and on climate data in Runge *et al* (2014), this feature helps to exclude the misleading effects of autocorrelation and external drivers.

The limitation is that such a multivariate model-free causal inference analysis demands much longer time series lengths than linear inference methods based on, for example, partial correlation since the properties of the whole joint distribution are taken into account rather than only the first two moments. In Runge (2014) the power of CMI as an independence test is studied and it was found that—for the Gaussian model class studied there—CMI tests have good power up to as much as 32-dimensional conditions for a sample length of at least 1000. Note that, due to the efficient iterative testing scheme of the causal algorithm, this dimension refers to the maximum number of parents in the causal graph and not to the number of processes, which can be much higher. On the other hand, for a low bias of MIT, as needed for a proper assessment of coupling strength, one should at most condition on about eight variables for 1000 samples to keep the relative error below about 30%, as further discussed in Runge (2014).

2.6. Bivariate symbolic coupling traces (SCT)

Another bivariate coupling measure, Symbolic Coupling Traces (SCT), developed by Wessel *et al* (2009), has been used to derive descriptive models of the cardiovascular system and its interactions. Here a further coarse graining of the beat-to-beat-interval based time series is performed via a symbolification of the time series by putting the symbol '1' whenever two consecutive values increase and '0' otherwise. From these symbol time series words of a certain length l (here $l = 3$) are built. Two of these word series are then shifted relative to each other by a lag τ, and the difference $\Delta T(\tau)$ of the occurrences of identical (symmetrical) words (e.g. 101 and 101) $T(\tau)$ and opposite (diametrical) words (e.g. 101 and 010) $\overline{T}(\tau)$ is computed. The lag shows the coupling direction, the sign of $\Delta T(\tau)$ the kind of coupling (symmetric/diametric), and the absolute value of $\Delta T(\tau)$ represents the coupling strength. According to Suhrbier *et al* (2010), the significance of the values of $\Delta T(\tau)$ is determined via an empirical significance threshold.

3. Results

We now analyze an ensemble of 13 datasets of healthy pregnant women and 10 women suffering from pre-eclampsia, as studied in Riedl *et al* (2010), where the measurements are described in more detail. The study was approved by the local ethics committee and it obtained the informed consent of all of the subjects. We use the time series (length 900, sampled at heart beats) of diastolic (D) and systolic (S) blood pressure, respiration (R), and intervals between successive heart beats (B). The time of the heart beats are defined by the R-peaks in the electrocardiogram. From the continuous blood pressure signal the local maxima, the systolic values, and the local minima, the diastolic values, were extracted, where the n-th systolic pressure is inside the n-th heart beat interval and the n-th diastolic pressure follows the n-th systolic one. The respiratory signal was resampled at the time instants of the R-waves by interpolation, where the n-th value is assigned to the second R-wave of the n-th interbeat interval.

3.1. Mutual information lag functions

First, we analyze the interactions using lagged mutual information, defined as

$$I_{XY}^{\mathrm{MI}}(\tau) \equiv I(X_{t-\tau}; Y_t)\,. \tag{7}$$

For $\tau > 0$, MI measures the information in the past of X that is contained in Y. In figure 2 we plot the lagged MIs for all healthy subjects as a matrix of lag functions instead of the common plot against positive and negative lags τ. The diagonal lag functions are, therefore, the auto-MI, defined as $I(Y_{t-\tau};Y_t)$ for $\tau > 0$ (for $\tau = 0$ this is the entropy $H(Y)$). In such a bivariate analysis all of the processes are found to be significantly associated. While one could draw some conclusions from the peaks (e.g. for the influence of diastolic on systolic blood pressure $D \to S$ at a lag of 1 or 2 (in units of heart beats)), lagged MI is not intended to yield a notion of causal direction.

3.2. Symbolic coupling trace analysis

By applying Bivariate Symbolic Coupling Traces (SCT) to the present data set one arrives at the coupling structure given in figure 3. As for MI also here we can identify different lags and it is also possible to identify contemporaneous links. While one can clearly find differences between the healthy group and the patients group suffering from pre-eclampsia, still, especially in the healthy group, we find many connections because the SCT—being a bivariate measure—does not account for information carried via a common driver. For example, the

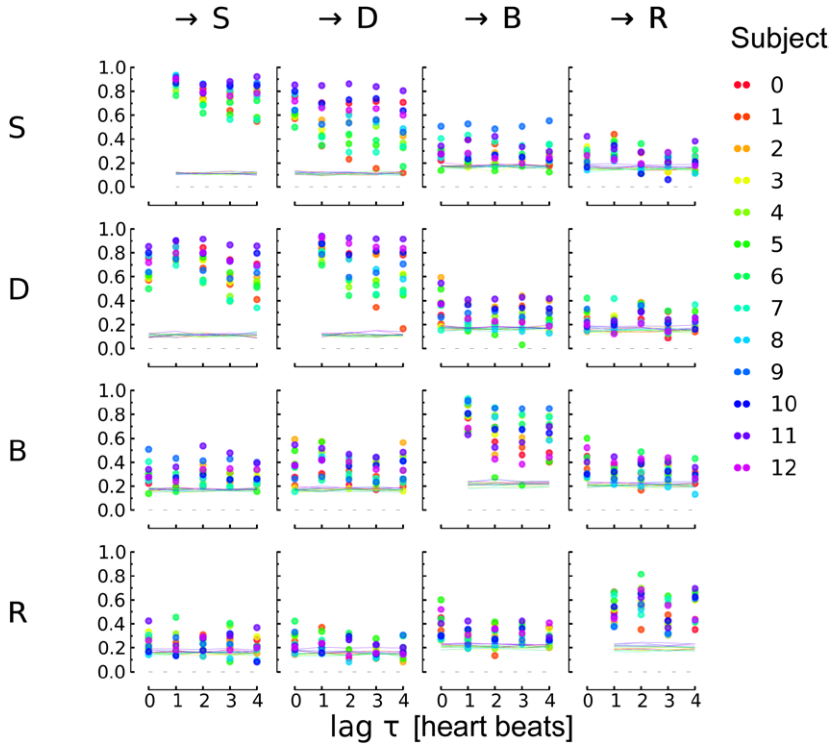

Figure 2. Lagged mutual informations between diastolic (D) and systolic (S) blood pressure, respiration (R), and heart beats (B) of 13 healthy pregnant women. The diagonal depicts the auto-MI functions (zero-lag not shown). We rescaled the CMI to the (partial) correlation scale via $I \to \sqrt{1 - \mathrm{e}^{-2I}} \in [0, 1]$ (Cover and Thomas 2006). The horizontal lines show shuffle significance test levels at $\alpha = 0.95$.

lag-2 link between B and S might be explained via the lag-1 links $B \to D$ and $D \to S$ (compared with figure 4).

3.3. Bivariate transfer entropy

Towards a causal interpretation, coupling measures need to be able to exclude information from a common past. Implementing this idea, Schreiber introduced *transfer entropy* (TE) (Schreiber 2000) which is the information-theoretic analogue of Granger causality. In the original article, TE was defined between two variables as

$$I^{\mathrm{TE}}_{X \to Y} \equiv I(X_t^{(l)}; Y_t | Y_t^{(m)}) \tag{8}$$

where $X_t^{(l)} = (X_{t-1}, \ldots, X_{t-l})$ (correspondingly for Y). TE is *not* lag-specific and measures the reduction in uncertainty about Y_t when learning the past of X_t, if the rest of the past of Y is already known. In practice this truncated TE is estimated with lag parameters $l = m = 1$ because higher dimensional CMIs are difficult to estimate, especially using discrete binning estimators. In figure 5 we show the TE-networks of all 13 healthy subjects overlaid. The link color denotes the ensemble average TE and the link width the fraction of subjects for which this TE value was significant (95% level). As in the MI analyses, we find all of the variables to be significantly mutually connected. Still, the strength of TE offers some room for

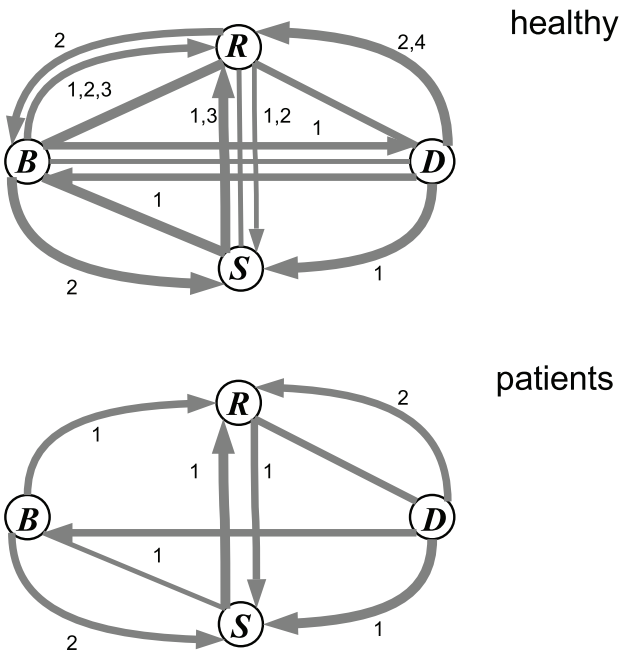

Figure 3. Bivariate coupling traces analysis (Wessel *et al* 2009) of healthy subjects and patients. The straight lines show the contemporaneous links and the curved arrows show the directed links. The link width corresponds to the percentage of ensemble members where this link was significant (the thickest line denote 100%, the thinnest lines about 50%).

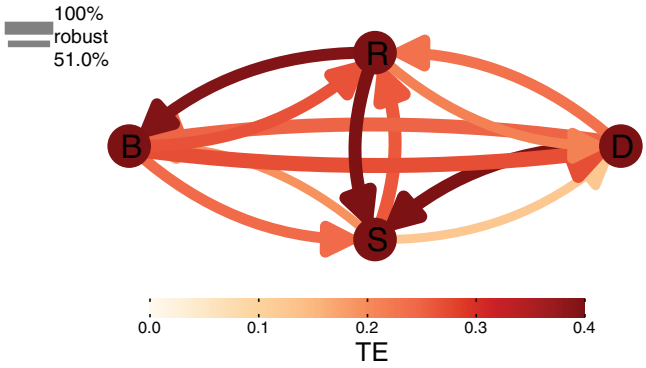

Figure 4. Bivariate transfer entropy analysis of the 13 healthy subjects. Colors denote the TE value (transformed to correlation scale). The link width denotes the percentage of ensemble members where this link was significant.

interpretations. For example, we observe strong TE values from the respiratory system to the heart rate and systolic blood pressure while the opposite directions are rather weak.

3.4. Momentary information transfer: case study

Now we move to a full multivariate causal analysis including coupling delays. The causal algorithm was run using a maximum delay of four heart beats (the maximum dimension in the

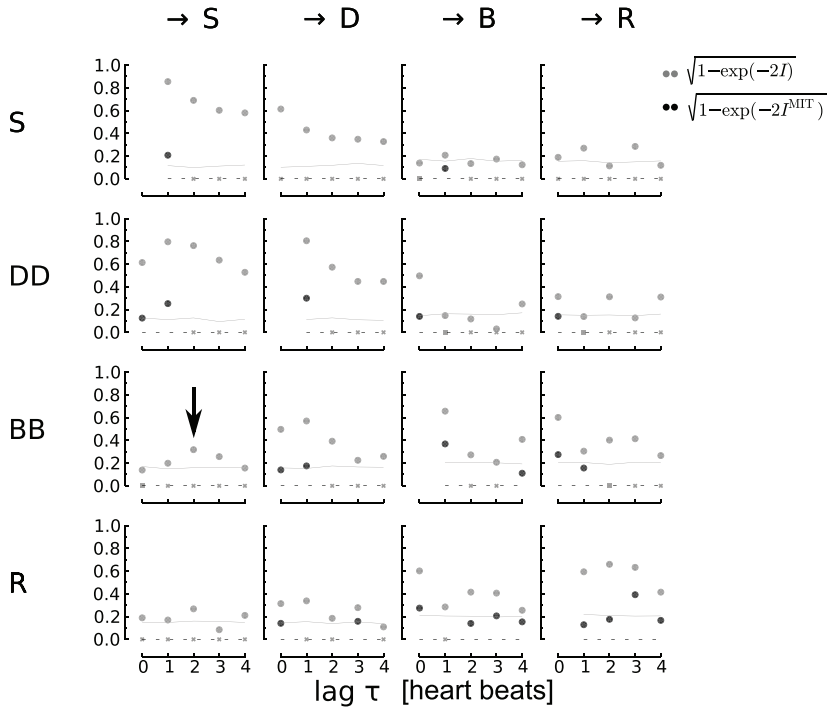

Figure 5. Mutual information lag functions (grey dots) and the associated 95% significance threshold (grey solid line). The black dots mark the significant MIT values of links that 'survived' the causal algorithm. Note that the grey line denotes the significance level only for MI. The fact that some MIT values are below this line is a consequence of the bias for the higher dimensional CMI and does not imply that the values are non-significant. Here the MI and MIT values are also transformed to the correlation scale.

n-loop in the algorithm) and conditioning on up to four parents (checking up to three different sets, the maximum in the i-loop). Significance at the 95% level was assessed using the shuffle test with 50 surrogates. CMI was estimated using $k = 100$ in the algorithm and $k = 10$ for MIT.

In figure 6 we analyze one of the healthy subjects. The MI lag functions are shown again for comparison. The couplings between diastolic and systolic blood pressure are shown in the upper left block, where one can see the effect of strong autodependencies on the MI estimate. The large and broad peak (grey), which is significant for both directions $D \to S$ and $S \to D$, shrinks to one significant coupling $D \to S$ at lag 1 with a much smaller MIT value (black) if one conditions on the parents of D and S. In Runge *et al* (2014) the authors investigate how strong autodependencies can shift even the maximum to larger lags, obscuring an assessment of a coupling delay. While here MI still somewhat indicates a causal link, the broad peak for the coupling $B \to S$ (arrow marker) vanishes upon conditioning on D. This represents a case where only a multivariate causal analysis unveils an indirect coupling mechanism $B \to D \to S$. This mechanism is also robustly found in the other subjects, as analyzed in the next section.

3.5. Momentary information transfer: comparison with patients

The analysis of all subjects is shown in figure 4 for both groups. We robustly find the causal chain $B \to D \to S$ in healthy subjects as well as patients with pre-eclampsia, which explains

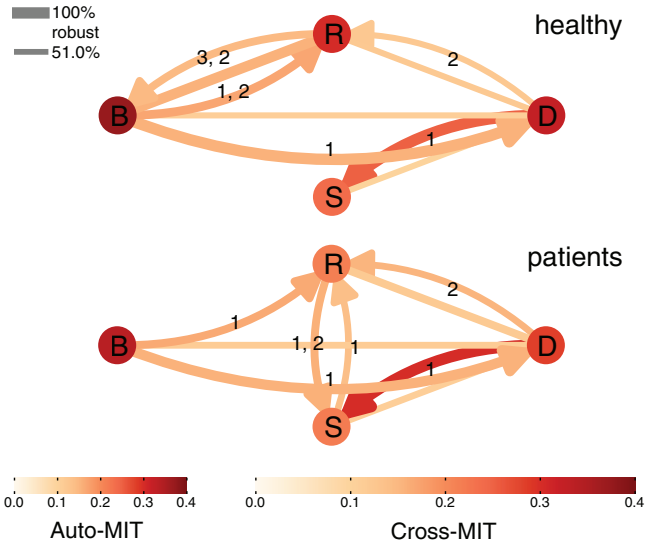

Figure 6. Causal interactions between diastolic (D) and systolic (S) blood pressure, respiration (R), and heart beats (B) of healthy pregnant women (top) and women suffering from pre-eclampsia (bottom). The colors and labels are described in figure 1(b), straight lines show contemporaneous links and curved arrows show directed links. The link width denotes the percentage of ensemble members where this link was significant.

the lagged influence of heart rate on systolic blood pressure found in the previous bivariate analyses using MI, SCT, and TE (also found in Nollo *et al* 2005, Porta *et al* 2002 and Wessel *et al* 2009). More precisely, Nollo *et al* (2005) and Porta *et al* (2002) detected causal coherence from B to S for both high frequencies and low frequencies. This causal chain $B \to D \to S$ also confirms the findings of Riedl *et al* (2010). There, $B \to D$ is explained by the influence of the stroke volume on the diastolic blood pressure, depending on heart rate. This relates to the 'Windkessel'-function of the aortic tree, which buffers about half of the stroke volume in order to decrease the differences of blood pressure during filling and ejection of the heart. This function also connects both diastolic and systolic blood pressure. The strength of connection is mainly determined by the elastic property of the aortic tree (compliance of the 'Windkessel'). Therefore, the different strength of $D \to S$ in both groups (figure 4) indicates a changed compliance, which confirms the results of Dart and Kingwell (2001).

Furthermore, consistent with Cohen and Taylor (2002), Faes *et al* (2006), Riedl *et al* (2010), Rosenblum *et al* (2002) and Stankovski *et al* (2013), we find that the link $R \to B$ (together with the contemporaneous link R–B) is less robust and, conversely, the links R–D and $R \to S$ are more robust for patients. In the case of $R \to S$, we find a difference in both groups, which is more clear than in Riedl *et al* (2010). This coupling seems to be the cause of larger respiratory induced fluctuations of the systolic blood pressure, which are used for the estimation of the baroreflex sensitivity in Malberg *et al* (2007) where pre-eclampsia leads to a significant increase.

The most significant differences to Riedl *et al* (2010) are $B \to R$ and $D \to R$ in both groups with a lag of 1 and 2 heart beats, respectively. Their higher lag indicates autonomic reflexes or integrations rather than mechanical mechanisms. The strongest mechanisms measured with MIT are the causal chain $B \to D \to S$ and the influences of B and D on R, where the latter is even stronger for patients, albeit not for all patients. A visual inspection, especially in the case of pre-eclampsia, shows a relation between heart rate rhythms of the very low frequency band

and modulations of the respiratory amplitude, which might be quantified by the found connection $B \to R$. The underlying mechanism of the very low frequency rhythms are unknown. Therefore, this frequency band is out of the scope of the traditional analysis of the heart rate variability. We only could find its consideration in cases of heart failure patients with periodic breathing where the heart rate's very low frequency is driven by the respiratory ones (Ponikowski *et al* 1999). A similar explanation might be given for the detected influences of the blood pressure values on respiration.

The absence of $S \to B$, which is also found in Riedl *et al* (2010), shows that these fluctuations may not be used for the quantification of the baroreflex because $S \to B$ is the mechanism of the baroreflex by definition. Rather, the aforementioned coupling $R \to B$ and the change of the peripheral resistance by means of respiratory modulations of the autonomic activity seems to be the cause of the variations in heart rate and blood pressure, see Cohen and Taylor (2002) and Stankovski *et al* (2013), respectively. In contrast to this result, bivariate close loop models show a causal coherence from S to B but only for high frequencies (Porta *et al* 2002, Nollo *et al* 2005). This finding indicates a flaw in the extraction of baroreflex sensitivity by means of standard sequence methods and spectral approaches based on high frequency power (Laude *et al* 2004). The contemporaneous connection of R and D that was detected in several subjects could be the result of a change of the intra-thoracic pressure filling the lungs, which leads to higher pressure on the 'Windkessel'. Note that these findings hold for baroreflex measurements under resting conditions.

4. Conclusions

We apply a recently introduced causal coupling inference approach to cardiovascular time series. Apart from assessing model-free information-theoretic causal associations including causal delays as important ingredients of a coupling mechanism, we also determine its strength in a meaningful way that attempts to exclude the misleading effects of autocorrelation and external dependencies. We have used this approach in conjunction with the model-free conditional mutual information but it can equivalently be utilized with the linear partial correlation (Runge *et al* 2014), which can be much easier estimated. In this preliminary application we confirm some of the causal mechanisms that were discussed in Riedl *et al* (2010) and find a possible explanation for the influence of heart rate on systolic blood pressure. This approach provides more precise insights into complex coupling structures and assists a more realistic physical interpretation. We also detected some unexpected couplings that might relate to slower rhythms than the ones considered in traditional heart rate analysis. This points towards a further improvement of the method by including different time delay embeddings to obtain a picture of scaled coupling patterns.

Acknowledgments

JR was supported by the German National Academic Foundation and AM by the DFG grant 'WE 2834/5-1'.

References

Bopp C M, Townsend D K, Warren S and Barstow T J 2014 Relationship between brachial artery blood flow and total (hemoglobin + myoglobin) during post-occlusive reactive hyperemia *Microvasc. Res.* **91** 37–43

Cammarota C and Rogora E 2006 Spectral and symbolic analysis of heart rate data during the tilt test *Phys. Rev.* E **74** 042903
Cohen M A and Taylor J A 2002 Short-term cardiovascular oscillations in man: measuring and modelling the physiologies *J. Physiol.* **542** 669–83
Cover T M and Thomas J A 2006 *Elements of Information Theory* (New York: Wiley)
Dahlhaus R 2000 Graphical interaction models for multivariate time series *Metrika* **51** 157–72
Dart A M and Kingwell B A 2001 Pulse pressure-a review of mechanisms and clinical relevance *J. Am. College Cardiol.* **37** 975–84
deBoer R W, Karemaker J M and Strackee J 1987 Hemodynamic fluctuations and baroreflex sensitivity in humans: a beat-to-beat model *Am. J. Physiol. Heart Circ. Physiol.* **253** H680–9
Dhamala M, Rangarajan G and Ding M 2008 Estimating Granger causality from Fourier and wavelet transforms of time series data *Phys. Rev. Lett.* **100** 018701
Eichler M 2012 Graphical modelling of multivariate time series *Probab. Theory Relat. Fields* **153** 233–68
Faes L, Cucino R and Nollo G 2006 Mixed predictability and cross-validation to assess non-linear Granger causality in short cardiovascular variability series *Biomed. Eng.* **51** 255–9
Frenzel S and Pompe B 2007 Partial mutual information for coupling analysis of multivariate time series *Phys. Rev. Lett.* **99** 204101
Granger C W J 1969 Investigating causal relations by econometric models and cross-spectral methods *Econometrica* **37** 424–38
Laude D, Elghozi J L, Girard A, Bellard E, Bouhaddi M, Castiglioni P, Cerutti C, Cividjian A, Di Rienzo M and Fortrat J O 2004 Comparison of various techniques used to estimate spontaneous baroreflex sensitivity (the EuroBaVar study) *Am. J. Physiol. Regul. Integr. Comp. Physiol.* **286** R226–31
Leistritz L, Pester B, Doering A, Schiecke K, Babiloni F, Astolfi L and Witte H 2013 Time-variant partial directed coherence for analysing connectivity: a methodological study *Phil. Trans. R. Soc.* A **371** 20110616
Malberg H, Bauernschmitt R, Voss A, Walther T, Faber R, Stepan H and Wessel N 2007 Analysis of cardiovascular oscillations: a new approach to the early prediction of pre-eclampsia *Chaos* **17** 015113
Marwan N, Romano M C, Thiel M and Kurths J 2007 Recurrence plots for the analysis of complex systems *Phys. Rep.* **438** 237–329
Nollo G, Faes L, Porta A, Antolini R and Ravelli F 2005 Exploring directionality in spontaneous heart period and systolic pressure variability interactions in humans: implications in the evaluation of baroreflex gain *Am. J. Physiol. Heart Circ. Physiol.* **255** H1777–85
Paluš M and Stefanovska A 2003 Direction of coupling from phases of interacting oscillators: an information-theoretic approach *Phys. Rev.* E **67** 055201
Paluš M and Vejmelka M 2007 Directionality of coupling from bivariate time series: How to avoid false causalities and missed connections *Phys. Rev.* E **75** 056211
Pompe B and Runge J 2011 Momentary information transfer as a coupling measure of time series *Phys. Rev.* E **83** 051122
Ponikowski P, Anker S D, Chua T P, Francis D, Banasiak W, Poole P A, Coats A J S and Piepoli M 1999 Oscillatory breathing patterns during wakefulness in patients with chronic heart failure: clinical implications and role of augmented peripheral chemosensitivity *Circulation* **100** 2418–24
Porta A, Baselli G, Rimoldi O, Malliani A and Pagani M 2000 Assessing baroreflex gain from spontaneous variability in conscious dogs: role of causality and respiration *Am. J. Physiol. Heart Circ. Physiol.* **279** H2558 –67
Porta A, Furlan R, Rimoldi O, Pagani M, Malliani A and van de Borne P 2002 Quantifying the strength of the linear causal coupling in closed loop interacting cardiovascular variability signals *Biol. Cybern.* **86** 241–51
Riedl M, Suhrbier A, Stepan H, Kurths J and Wessel N 2010 Short-term couplings of the cardiovascular system in pregnant women suffering from pre-eclampsia *Phil. Trans. R. Soc.* A **368** 2237–50
Rosenblum M G, Cimponeriu L, Bezerianos A, Patzak A and Mrowka R 2002 Identification of coupling direction: application to cardiorespiratory interaction *Phys. Rev.* E **65** 041909
Runge J 2014 Detecting and quantifying causality from time series of complex systems *PhD Thesis* Humboldt University, Berlin
Runge J, Heitzig J, Marwan N and Kurths J 2012a Quantifying causal coupling strength: a lag-specific measure for multivariate time series related to transfer entropy *Phys. Rev.* E **86** 061121

Runge J, Heitzig J, Petoukhov V and Kurths J 2012b Escaping the curse of dimensionality in estimating multivariate transfer entropy *Phys. Rev. Lett.* **108** 258701

Runge J, Petoukhov V and Kurths J 2014 Quantifying the strength and delay of climatic interactions: the ambiguities of cross correlation and a novel measure based on graphical models *J. Climate* **27** 720–39

Schelter B O, Winterhalder M, Dahlhaus R, Kurths J and Timmer J 2006 Partial phase synchronization for multivariate synchronizing systems *Phys. Rev. Lett.* **96** 20

Schreiber T 2000 Measuring information transfer *Phys. Rev. Lett.* **85** 461–4

Schulz S, Adochiei F-C, Edu I-R, Schroeder R, Costin H, Bär K-J and Voss A 2013 Cardiovascular and cardiorespiratory coupling analyses: a review *Phil. Trans. R. Soc.* A **371** 20120191

Spirtes P and Glymour C 1991 An algorithm for fast recovery of sparse causal graphs series *Soc. Sci. Comput. Rev.* **9** 62–72

Spirtes P, Glymour C and Scheines R 2000 *Causation, Prediction and Search* (Cambridge, MA: MIT Press)

Stankovski T, Cooke W H, Rudas L, Stefanovska A and Eckberg D L 2013 Time-frequency methods and voluntary ramped-frequency breathing: a powerful combination for exploration of human neurophysiological mechanisms *J. Appl. Physiol.* **155** 1806–21

Suhrbier A, Riedl M, Malberg H, Penzel T, Bretthauer G, Kurths J and Wessel N 2010 Cardiovascular regulation during sleep quantified by symbolic coupling traces *Chaos* **20** 045124

Wessel N, Suhrbier A and Riedl M 2009 Detection of time-delayed interactions in biosignals using symbolic coupling traces *Europhys. Lett.* **87** 10004